Imaging Assessment of Visceral Pleural Surface Invasion by Lung Cancer: Comparison of Computed Tomography and Contrast-enhanced Radial T1-weighted Gradient Echo 3-Tesla Magnetic Resonance Imaging

Yu Zhang

The Graduate School

Yonsei University

Department of Medicine

Imaging Assessment of Visceral Pleural Surface Invasion by Lung Cancer: Comparison of Computed Tomography and Contrast-enhanced Radial T1-weighted Gradient Echo 3-Tesla Magnetic Resonance Imaging

Directed by Professor Sung Min Ko

A Dissertation Submitted to the Department of Medicine and the Graduate School of Yonsei University in Partial Fulfillment of the Requirements for the Degree of Doctor of Philosophy

Yu Zhang

June 2021

This certifies that the Doctoral Dissertation of

Yu Zhang is approved.

_____

Thesis Supervisor: Sung Min Ko

_____

Sang-Ha Kim: Thesis Committee Member

_____

Won-Yeon Lee: Thesis Committee Member

_____

Suk Joong Yong: Thesis Committee Member

_____

Soon-Hee Jung: Thesis Committee Member

The Graduate School,

Yonsei University

June 2021

ACKNOWLEDGEMENT

First of all, I would like to express my heartfelt gratitude to my supervisor Professor Sung Min Ko who gave me the opportunity to challenge the Joint degree in Yonsei University, a world-renowned university. Professor Sung Min Ko has advised me with his invaluable insight, rigorous academic attitude, excellence in work style, frequent encouragement, and endless support throughout my joint courses, clinical training, and research. Over the past four years, professor Sung Min Ko has used his wisdom, professionalism, humorand kindness to impact and inspire me to move forward step by step in this university and in this country. It is knowledgeable and responsible that gave me careful guidance in my studies and research. He cared for me in life and created a relaxed environment for me.

Secondly, I especially thank Professor Jung Ja Lee who have given me a lot of helps as long as my stay in Korea. I have always received care and kindness from her. I would also like to express my sincere gratitude to the members of my dissertation committee, including Professor Sang-Ha Kim, Professor Won-Yeon Lee, Professor Suk Joong Yong and Professor Soon-Hee Jung for their valuable advices and instructions. They have profound and professional knowledge, much research

experience in different academic fields. They not only taught us the relevant courses but also effectively guided my research work, so that my research capabilities continued to improve.

Thirdly, I sincerely gratefully thank Professor Jeanne B. Ackman, Professor Woocheol Kwon, Professor Ho Yun Lee who are from Harvard Medical School, Ewha Womans University and Sungkyunkwan University, they gave me helpful guidance during my joint degree studies and research, from the topic selection of the thesis, patient data, the writing of the thesis to the final draft. Their profound and extensive professional knowledge, serious and responsible work attitude, and rigorous and realistic academic spirit have made my thesis be fully affirmed.

Fourthly, I would like to thank the professors and the members of the department of Radiology and related clinical departments in the Wonju Severance Christian Hospital for their high-level clinical technique, teaching technology and abundant symposium discussion that make me better and better. They provided me with a very favorable clinical medical training environment from different perspectives, which enabled me to access and learn precise clinical thinking and advanced clinical technology.

Fifthly, I would like to express my sincere gratitude to all the schoolmates and

friends in my studying career. No matter in study or life, they have given me selfless help and enthusiastic care, allowing me to spend the past years in a warm environment.

Finally, yet importantly, I feel a deep sense of gratitude to my parents and boyfriend whose love me. Thank my father and mother for giving me life, care, diligent and wisdom, leading me to be useful to society. Thank my boyfriend who is my future husband for giving me accompany, understanding and encouragement. With your support and concern, I can always get out of the trough of frustration and rush to the battlefield known as the future.

June, 2021

Yu Zhang

CONTENT

List of Figures

List of Table

ABSTRACT

Imaging Assessment of Visceral Pleural Surface Invasion by Lung Cancer: Comparison of CT and Contrast-Enhanced Radial T1-Weighted Gradient Echo 3-Tesla MRI

Yu Zhang

Department of Medicine

The Graduate School, Yonsei University

Directed by Professor Sung Min Ko

Objective: To compare the diagnostic performance of contrast-enhanced radial T1-weighted gradient-echo 3-tesla (3T) magnetic resonance imaging (MRI) and computed tomography (CT) for the detection of visceral pleural surface invasion

(VPSI). Visceral pleural invasion by non-small-cell lung cancer (NSCLC) can be classified into two types: PL1 (without VPSI), invasion of the elastic layer of the visceral pleura without reaching the visceral pleural surface, and PL2 (with VPSI), full invasion of the visceral pleura.

Materials and Methods: Thirty-three patients with pathologically confirmed VPSI by NSCLC were retrospectively reviewed. Multidetector CT and contrast-enhanced 3T MRI with a free-breathing radial three-dimensional fat-suppressed volumetric interpolated breath-hold examination (VIBE) pulse sequence were compared in terms of the length of contact, angle of mass margin, and arch distance-to-maximum tumor diameter ratio. Supplemental evaluation of the tumor-pleura interface (smooth versus irregular) could only be performed with MRI (not discernible on CT).

Results: At the tumor-pleura interface, radial VIBE MRI revealed a smooth margin in 20 of 21 patients without VPSI and an irregular margin in 10 of 12 patients with VPSI, yielding an accuracy, sensitivity, specificity, positive predictive value, negative predictive value, and F-score for VPSI detection of 91%, 83%, 95%, 91%, 91%, and 87%, respectively. The McNemar test and receiver operating characteristics curve

analysis revealed no significant differences between the diagnostic accuracies of CT and MRI for evaluating the contact length, angle of mass margin, or arch distance-to-maximum tumor diameter ratio as predictors of VPSI.

Conclusion: The diagnostic performance of contrast-enhanced radial T1-weighted gradient-echo 3T MRI and CT were equal in terms of the contact length, angle of mass margin, and arch distance-to-maximum tumor diameter ratio. The advantage of MRI is its clear depiction of the tumor-pleura interface margin, facilitating VPSI detection.

Keywords: Magnetic resonance imaging; Lung cancer; Diagnostic imaging

Imaging Assessment of Visceral Pleural Surface Invasion by Lung Cancer: Comparison of CT and Contrast-Enhanced Radial T1-Weighted Gradient Echo 3-Tesla MRI

Yu Zhang

Department of Medicine

The Graduate School, Yonsei University

Directed by Professor Sung Min Ko

I. INTRODUCTION

Visceral pleural invasion (VPI) by non-small-cell lung cancer (NSCLC) can be classified into two types, PL1 and PL2, representing cases without and with visceral pleural surface invasion (VPSI), respectively (1-3). The 8th edition of the TNM classification for lung cancer classifies both invasion of the elastic layer of the visceral pleura without reaching the visceral pleural surface (PL1) and full invasion

of the visceral pleura (PL2) as stage T2 (4), suggesting that PL1 and PL2 tumors have similar prognosis and survival (5). However, a study showed that the 5-year overall survival rate was significantly higher for patients with PL1 tumors (61.9%) than for those with PL2 tumors (39.2%) (6), PL1 tumors (63.7%) than for those with PL2 tumors (49.6%), respectively, with significant differences between PL1 and PL2 (7) ($p< 0.0001$ and $p= 0.002$). The 5-year survival rates of patients with and without VPSI were 57.9% and 83.0%, respectively ($p = 0.001$), for N0–N2 disease and 74.3% and 88.5%, respectively ($p = 0.005$), for N0 disease (1). VPSI might therefore be considered an independent risk factor for poor prognosis, and its presence might be a potential indication for adjuvant chemotherapy (1, 8).

Chest radiography (CXR) is the most common diagnostic imaging tool for lung disease, however, CXR is not suitable for evaluating pleural invasion in early stage (9).Ultrasound (US) is a widely used and low-cost non-invasive tool, however, it is difficult to predict VPI by using US (10, 11).

Computed tomography (CT) is a noninvasive imaging modality for preoperative staging of lung cancers. However, it has limitations in the detection of more subtle cases of pleural invasion, as contiguity of the tumor with the pleural surface is not

necessarily equivalent to its invasion (12, 13). Most published have been shown to have predictive value for pleural invasion, Kawaguchi et al. (14) indicated that tumor invasion beyond the parietal pleura on CT and complaints of chest pain were independent indicators of invasion into the chest wall (15). Shimada et al. showed the combination of a tumor disappearance ratio (TDR) larger than 0.5 and the absence of spiculation was highly predictive of noninvasion or minimally invasion in T1aN0M0 peripheral NSCLC (16). Similar to TDR, consolidation-to-tumor ratio (CTR) may also be indicated for predicting only tumor invasion, could not predict pleural invasion precisely (17). A skirt-like 3-dimensional (3D) CT pattern of pleural morphology adjacent to the tumor was shown to be more accurate than other 3D pleural patterns for predicting pleural invasion, with an accuracy of 77%. However, the effort required to construct 3D-rendered images and calculate the R_{area} is time-intensive (18), pleural tag with a soft tissue component with a soft tissue component provided moderate evidence of VPI, with 70.8% accuracy (19), and type-5 border (convex border with a perpendicular or blunt angle) , which was one of 5 types assessed by lung windows for maximal pleural attachment, was considered a moderate indicator of pleural invasion, with 57% accuracy (20)， high-resolution computed tomography (HRCT) findings and fluorine-18-fluorodeoxyglucose (18F-

FDG) uptake (^{18}F-FDG PET/CT) was also used for predicting VPI according to the maximum standardized uptake value (SUVmax) (9), however, these methods cannot be used to differentiate PL1 from PL2.

Magnetic resonance imaging (MRI) is potentially advantageous for VPSI detection because of its superior soft tissue contrast and tissue characterization properties, without ionizing radiation exposure. Conventional MRI can yield high-quality images of the thorax, particularly with breath-hold techniques; however, breath-holding can be challenging for some patients. Free-breathing, intravenous contrast-enhanced, radial, 3D ultrafast gradient-echo (volumetric interpolated breath-hold examination [VIBE]) T1-weighted imaging, hereinafter referred to as “radial VIBE,” has been proposed as an alternative to breath-hold post-contrast imaging. It enables patients to breathe freely during scanning, yielding excellent image quality and diagnostic performance owing to the enhanced lesion conspicuity, clarity of the tumor interface, and reduced respiratory motion artifacts compared to other free-breathing techniques (21-26). It would be of value to ascertain whether CT and MRI can distinguish between PL1 and PL2 and thereby assist in selection of appropriate lung cancer therapy.

Moreover, this sequence has been proven to be useful for evaluating the morphological features of lung cancer and for readily demonstrating the tumor-pleura interface (27). Therefore, this study aimed to compare the diagnostic performance of contrast-enhanced, radial VIBE 3-Tesla (3T) MRI, and CT for VPSI detection.

II. MATERIALS AND METHODS

This retrospective, bi-institutional study was conducted at Wonju Severance Christian Hospital and Samsung Medical Center. The study was approved by the institutional review boards of both institutions and the local ethics committee (IRB No. CR319094). The requirement for written informed consent was waived.

1. Patients

Initially, 191 consecutive lung cancer patients who underwent both CT and 3T MRI between January 2016 and May 2019 were enrolled. Patients with poor quality CT or MRI scans were excluded (Figure 1). Finally, a total of 33 patients met the

following inclusion criteria: (1) nonmetastatic, primary NSCLC treated with surgical resection, (2) available pathology reports describing the extent of pleural invasion, (3) preoperative CT and 3T MRI scans with the same scan parameters available on a picture archiving and communication system (PACS); (4) available free-breathing fat-saturated radial VIBE sequence on MRI; (5) suspected pleural invasion on CT; (6) CT and MRI performed within 3 months; and (7) no prior or current chemotherapy or radiation therapy. The sample including 23 patients from the Blinded Hospital and 10 from the Blinded Medical Center was comprised of 28 men and five women, aged 46–88 years (mean age, 68 ± 10 years). This study analyzed 17 adenocarcinomas, 13 squamous cell carcinomas, and three large cell carcinomas (Table 1).

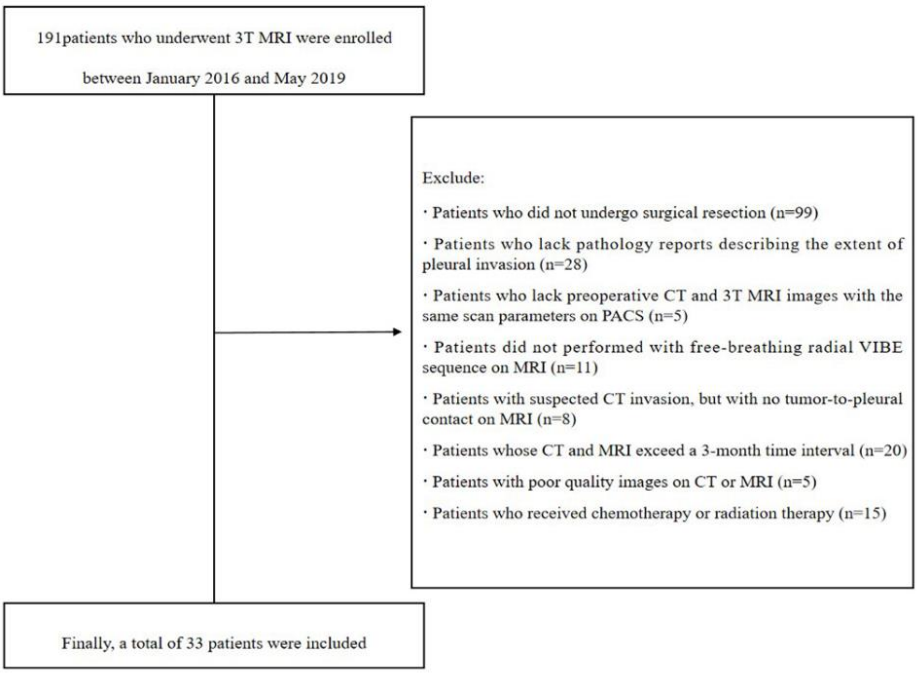

Fig. 1. Flowchart illustrating patient selection. CT = computed tomography, MRI = magnetic resonance imaging, NSCLC = non-small cell lung cancer, PACS = picture archiving and communication system, VIBE = volumetric interpolated breath-hold examination, 3T = 3-tesla

Table 1. Clinicopathologic Features of Non-Small-Cell Lung Cancer Patients in This Study

Clinicopathologic Features	Data
No. of patients	33
Age, years, mean ± SD (46–88)	68.33±9.96
Sex, n (%)	
Male	28 (84.8)
Female	5 (15.2)
Tumor size, mm, mean ± SD	53.4±26.2
Tumor pathology, n (%)	
Adenocarcinoma	17 (51.5)
Squamous cell carcinoma	13 (39.4)
Large cell carcinoma	3 (9.1)
Tumor location, n (%)	
RUL	11 (33.3)
RML	1 (3.0)
RLL	12 (36.4)
LUL	3 (9.1)
LLL	6 (18.2)
T stage, n (%)	
T1	1 (3.0)
T2	14 (42.4)
T3	12 (36.4)
T4	6 (18.2)
Pleural invasion grade, n (%)	
PL0	11 (33.3)
PL1	10 (30.3)
PL2	3 (9.1)
PL3	9 (27.3)

LLL = left lower lobe, LUL = left upper lobe, RLL = right lower lobe, RML = right middle lobe, RUL = right upper lobe

2. CT scanning

A 64-channel multidetector CT scanner (Brilliance 64, Philips Medical System, Cleveland, OH, USA) was used at both institutions for breath-hold imaging in the supine position, with a 7–8 second breath-hold. The technical parameters of the CT scans were as follows: 0.625-mm detector collimation, 512 × 512 matrix, 340-mm field-of-view, 80–120-mAs tube current, 120-kV tube voltage, 2.5-mm slice thickness, and 0.5-s rotation time. For each patient, 350 mg/mL iohexol contrast material was administered intravenously at a rate of 2.5 cc/s (27).

3. MRI

All MRI examinations were performed using a 3T system (MAGNETOM Skyra, Erlangen, Germany) with a 60-channel body coil. Patients were imaged in the supine position with their arms overhead to eliminate potential artifacts from the arms positioned on each side. The following pulse sequences were used in 23 patients: axial breath-hold T1- and T2-weighted turbo spin echo, axial T2-weighted half-Fourier acquisition single-shot turbo spin echo, contrast-enhanced fat-saturated T1-

weighted, and contrast-enhanced free-breathing, fat-saturated radial VIBE. The pulse sequences common to all included patients were breath-hold T1-weighted and contrast-enhanced free-breathing fat-suppressed radial VIBE. Gadoteridol (0.1 mmol/kg; Pro-Hance; Bracco Imaging, Milano, Italy) was injected at a rate of 1.5 cc/s. The radial VIBE imaging parameters with an isotropic resolution of 0.9 mm were as follows: repetition time, 3.36 ms; echo time, 1.66 ms; flip angle, 5°; field of view, 260 mm × 260 mm; and matrix size, 288 × 288 mm.

4. Imaging analysis

Two chest radiologists (readers 1 and 2, with 23 and 3 years of clinical experience, respectively), who were blinded to the patients' clinical information and pathological results, evaluated the CT and MRI scans by consensus. To make the final decision, the radiologists were allowed to refer to the images several times and adjust the window and level settings if necessary. The observers were instructed to read all CT scans first, followed by MRI scans after 1 month to avoid interference bias between CT and MRI results in interpretation.

Tumor size (maximum dimension in any of the three planes [axial, sagittal, and coronal]) on CT and MRI scans, and tumor location were recorded. The angle of the mass margin was formed from the center of the tumor toward both ends of the pleural contact. The length of pleural contact was the length of the interface between the primary tumor and the pleura. It was drawn freehand and measured in the same image (Figure 2B) (28, 29). The arch distance to maximum tumor diameter ratio was the length of the interface between the primary tumor and the neighboring structure (in this case, the pleura) (Figure 2B) (30). The imaging criteria utilized to determine the degree of suspicion for VPI were as follows (Figure 2A): A high suspicion for VPI required a length of pleural contact > 5 cm or a > 180° angle between the margin of the mass and the pleural surface; moderate suspicion of VPI required a 3–5 cm contact length or a 90°–180° angle between the mass and the pleural surface; and mild suspicion of pleural invasion required a length of pleural contact < 3 cm or angle of mass margin < 90°.

A. B.

Fig 2. Measurement of the angle between the margin of the mass and the pleural surface and arch distance-to-maximum tumor diameter ratio on the CT images.

(A) Measurement of the angle between the margin of the mass and the pleural surface on computed tomography (CT). The length of pleural contact was drawn freehand. The angle formed by the center of the mass and the two ends of the length of pleural contact is the "angle of mass margin." (B) Measurement of the arch distance-to-maximum tumor diameter ratio on the CT image of a pathologically determined PL2. Arch distance is defined as the length of the interface between the primary tumor and a neighboring structure, which, in this case, is the pleura (14). The arch distance was drawn freehand and measured in the same image.

Subsequently, the arch distance-to-maximum tumor diameter ratio was calculated.

CT = computed tomography

Based on the smoothness or irregularity of the high signal intensity band interface between the tumor and the pleura, MRI scans were classified into two groups (Figure 3): without VPSI, with smooth and clear margins, well-defined curvilinear pleural enhancement, and absence of protrusion of the interface between the tumor and the pleura (Figure 3A); and with VPSI, with an irregular, undulating, or coarse margin or protrusion of the interface between the primary tumor and the pleura (Figure 3B). The two groups were assessed in the axial, sagittal, and coronal planes. VPSI was determined if an irregular interface was observed in any plane. The lung cancer was deemed to be without VPSI only when there was a smooth tumor-pleura interface in all three planes.

A. B.

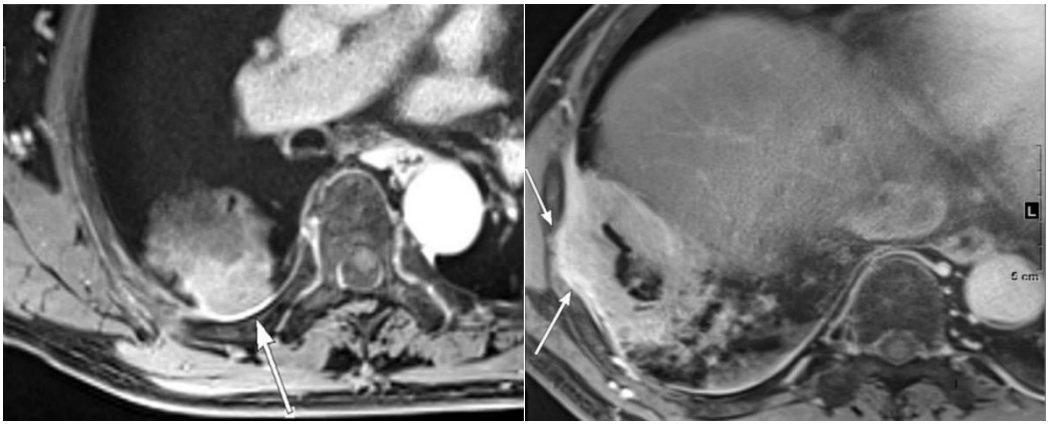

Fig. 3. Lung cancer without and with visceral pleural surface invasion (VPSI).

(A) Right lower lobe lung adenocarcinoma without VPSI in a 69-year-old woman shows a smooth and clear margin, with well-defined curvilinear pleural enhancement (arrow) and absence of protrusion of the tumor into the pleura. (B) Right lower lobe squamous cell carcinoma with VPSI in a 76-year-old man shows an irregular, undulating, or coarse margin or protrusion of the tumor (arrow) at the interface between tumor and pleura

5. Pathological analysis

Pathological specimens were stained with the Verhoeff-Van Gieson stain to investigate the presence and extent of pleural invasion. A pathologist with 33 years of experience in analyses of lung specimens performed the analysis and staged the pleural invasion in each patient as follows: PL0, no pleural invasion; PL1, tumor invasion beyond the elastic layer of the visceral pleura but not the surface of the visceral pleura; PL2, tumor invasion of the surface of the visceral pleura; and PL3, tumor invasion of the parietal pleura or chest wall (31).

6. Statistical analysis

Patient age and tumor size were assessed using the Wilcoxon rank-sum test. Sex, tumor pathology, and tumor location were assessed using Fisher's exact test between the two groups. Kappa statistics for categorical data were used to determine interobserver agreement. The Kappa result was interpreted as follows: < 0.20, slight; 0.21.0.40, fair; 0.41.0.60, moderate; 0.61.0.80, substantial; and > 0.81, excellent (32). The chi-square or Fisher's exact test for categorical data and Wilcoxon rank-sum test

for continuous data were used to examine the significant differences between patients with and without VPSI. A p-value < 0.05 was considered statistically significant. The diagnostic accuracy, sensitivity, specificity, positive predictive value (PPV), negative predictive value (NPV), and F-score were calculated separately. The accuracies of MRI and CT for evaluating the length of contact and arch distance to maximum tumor diameter ratio were compared using the McNemar test. The receiver operating characteristic (ROC) curve analysis was used to assess the diagnostic values of CT and MRI for VPSI detection, and the area under the curve was calculated. All data analyses were performed using the Statistical Analysis System (SAS) version 9.4 (SAS Institute Inc., Cary, NC, USA).

III. RESULTS

The histopathological diagnoses of NSCLCs were as follows: 17 adenocarcinomas, 13 squamous cell carcinomas, and three large cell carcinomas. There were 11 tumors in the right upper lobe, one in the right middle lobe, 12 in the right lower lobe, three

in the left upper lobe, and six in the left lower lobe (Table 1).

There were 21 patients without VPSI and 12 patients with VPSI, as determined pathologically. The mean and median tumor size of lung cancer were 49.7 ± 17.9 mm and 44 (33–55) mm, respectively, in the group without VPSI and 61.6 ± 24.2 mm and 55 (38.5–85) mm, respectively, in the group with VPSI. Although a larger tumor diameter was observed in patients with VPSI than in those without, tumor size was not significantly different between the two groups ($p = 0.170$). There was no significant difference between the two groups in patient age, sex, tumor pathology, or tumor location (Table 2). Tables 3 and 4 show the p-value, accuracy, sensitivity, specificity, PPV, NPV, and F-score for the length of contact, angle of mass margin, and arch distance-to-maximum on CT and MRI. The McNemar test showed no significant difference ($p > 0.05$) in the accuracy of the contact length (MRI, 67%; CT, 61%), angle of mass margin > 90° (both MRI and CT, 61%), or arch distance to maximum tumor diameter ratio > 0.9 (CT, 67%; MRI, 61%) between CT and MRI (Table 5). Moreover, there was no significant difference in the area under the ROC curve for VPSI detection between CT and MRI, suggesting that the diagnostic performances of CT and MRI were similar (Figure 4) regarding these characteristics.

Table 2. Comparison of Clinicopathologic Features of Non-Small-Cell Lung Cancer Patients Without and with Visceral Pleural Surface Invasion

Variables	Without VPSI †	With VPSI ‡ (n=12)	*p*-value
Age, years, median (Q1–Q3)	72 (64–77)	65 (54–73)	0.0600
Sex, n (%)			
Male	16 (76.2)	12 (100.0))	0.1329*
Female	5 (23.8)	0 (0.0)	
Tumor size (mm), median	44 (33–55)	55 (38.5–85)	0.1696
Tumor pathology, n (%)			
Adenocarcinoma	12 (57.1)	5 (41.6)	0.2149*
Squamous cell	8 (38.1)	5 (41.7)	
Large cell carcinoma	1 (4.8)	2 (16.7)	
Location, n (%)			
RUL	6 (28.6)	5 (41.7)	0.1057*
RML	1 (4.8)	0 (0.0)	
RLL	9 (42.9)	3 (25.0)	
LUL	0 (0.0)	3 (25.0)	
LLL	5 (23.8)	1 (8.3)	

*Fisher's exact test

†includes PL0 and PL1

‡includes PL2 and PL3

LLL = left lower lobe; LUL = left upper lobe; RLL = right lower lobe; RML = right middle lobe; RUL = right upper lobe; VPSI = visceral pleural surface invasion

Table 3. Computed Tomography and Magnetic Resonance Imaging Findings in Non-Small-Cell Lung Cancer Patients Without and with Visceral Pleural Surface Invasion

Variables / Pathology	Without VPSI* (n=21)	With VPSI†(n=12)	*p*-value
Tumor size, mm, median (Q1–Q3)			
CT	44 (32.1–54.9)	51 (41.7–82.7)	0.1593
MRI	45 (34.6–60.3)	54 (44.2–77.9)	0.1646
Length of contact, n (%)			
CT			
≤3 cm	10 (47.6)	2 (16.7)	0.1330*
>3 cm	11 (52.4)	10 (83.3)	
≤5 cm	16 (76.2)	6 (50.0)	0.1490*
>5 cm	5 (23.8)	6 (50.0)	
MRI			
≤3 cm	10 (47.62)	0 (0.0)	0.0050*
>3 cm	11 (52.38)	12 (100.0)	
≤5 cm	15 (71.4)	6 (50.0)	0.2743
>5 cm	6 (28.6)	6 (50.0)	
Angle of mass margin, n (%)			
CT			
≤90°	8 (38.1)	0 (0.0)	0.0299*
>90°	13 (61.9)	12 (100.0)	
≤180°	20 (95.2)	10 (83.3)	0.5381*
>180°	1 (4.8)	2 (16.7)	
MRI			
≤90°	8 (38.1)	0 (0.0)	0.0299*
>90°	13 (61.9)	12 (100.0)	
≤180°	20 (95.2)	10 (83.3)	0.5381*
>180°	1 (4.8)	2 (16.7)	
Arch distance-to-maximum tumor			
CT			
≤0.9	13 (61.9)	3 (25)	0.0413
>0.9	8 (38.1)	9 (75)	
MRI			
≤0.9	12 (57.1)	4 (33.3)	0.1880
>0.9	9 (42.9)	8 (66.7)	
Interface between the primary			
Smooth and clear margin	20 (95.2)	2 (16.7)	<.0001*
Irregular or coarse margin	1 (4.8)	10 (83.3)	

*includes PL0 and PL1, †includes PL2 and PL3

Table 4. Comparison of Computed Tomography and Magnetic Resonance Imaging Findings for Prediction of Visceral Pleural Surface Invasion, with Pathology as the Reference Standard

Variables	Accuracy	Sensitivity	Specificity	PPV	NPV	F-score	Kappa
Length of contact							
CT							
> 3 cm	61	83	48	48	83	61	0.2667
> 5 cm	67	50	76	55	73	52	0.2667
MRI							
> 3 cm	67	100	48	52	100	69	0.3980
> 5 cm	64	50	71	50	71	50	0.2143
Angle of mass margin							
CT							
> 90°	61	100	38	48	100	65	0.3092
> 180°	67	17	95	67	67	27	0.1418
MRI							
> 90°	61	100	38	48	100	65	0.3092
> 180°	67	17	95	67	67	27	0.1418
Arch distance-to-maximum							
CT (> 0.9)	67	75	62	53	81	62	0.3388
MRI (> 0.9)	61	67	57	47	75	55	0.2186
Interface							
MRI	91	83	95	91	91	87	0.8000

CT = computed tomography; MRI = magnetic resonance imaging; NPV = negative predictive value; PPV = positive predictive value

Table 5. Agreement Between Radial Volumetric Interpolated Breath-Hold Examination Magnetic Resonance Imaging and Computed Tomography When the Same Methods Were Employed

Variables	Kappa Coefficient	McNemar test
Length of contact (> 3 cm)	0.7284	0.3173
Length of contact (> 5 cm)	0.9333	0.3173
Angle of mass margin (> 90°)	1.0000	-
Angle of mass margin (> 180°)	1.0000	-
Arch distance-to-maximum tumor diameter ratio (> 0.9)	0.8787	> 0.9999

A. B. C.

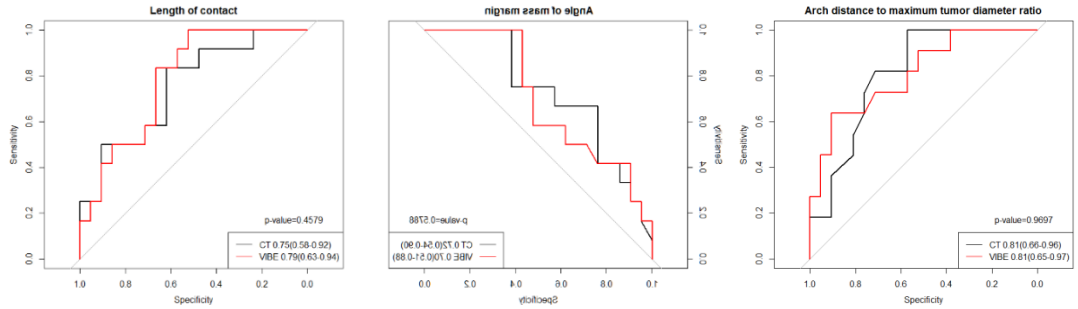

Fig. 4. Summarized receiver operating characteristic curves demonstrating the area under the curve of 75% (95% CI: 58–92%), 72% (95% CI: 54–90%), 81% (95% CI: 66–96%) for CT and 79% (95% CI: 63–94%), 70% (95% CI: 51–88%), 81% (95% CI:65–97%) for magnetic resonance imaging in the diagnosis of visceral pleural surface invasion on length of contact (A), angle of mass margin (B) and arch distance to maximum tumor diameter ratio (C), respectively. CI = confidence interval, CT = computed tomography, VIBE = volumetric interpolated breath-hold examination

Examination of the high-signal-intensity band interface between the tumor and the pleura on MRI revealed a smooth margin in 20 of 21 (95.2%) patients without VPSI and an irregular or coarse margin in 10 of 12 (83.3%) patients with VPSI. Similar signs in patients with and without VPSI were not appreciable on CT (Figures 3 and 5). The interface on MRI with the radial VIBE sequence significantly differed between patients with and without VPSI ($p < 0.001$) (Table 3), and sensitivity, specificity, accuracy, PPV, NPV, and F-score were 83%, 95%, 91%, 91%, 91%, and 87%, respectively. The Kappa value of the comparison between the pathology and MRI was substantial at 0.800 for the radial VIBE sequence (Table 4)

IV. DISCUSSION

This study showed that contrast-enhanced 3T MRI with the free-breathing fat-saturated radial VIBE sequence was superior to CT in depicting and distinguishing NSCLCs without VPSI from those with VPSI. VPSI is an independent factor for the poor prognosis of patients with NSCLCs and can influence the T stage, treatment, and prognosis (5). Therefore, determining VPSI and the depth of pleural invasion is

important (18). To predict pleural invasion, several radiological tools have been used in recent years. Chest radiography, which is the most common modality for the initial investigation of lung disease, is unsuitable for the assessment of pleural invasion (15). Although CT is widely used for staging lung cancers, its ability to predict pleural invasion is limited (2). Dynamic free-breathing steady-state free precession MRI has been used to assess the movement of a tumor abutting the chest wall during breathing with 88.5% accuracy (33). The whole-lesion histogram analysis of the apparent diffusion coefficient could assist in the assessment of pleural invasion (34). However, to the best of our knowledge, no previous studies have distinguished PL1 from PL2 pleural invasion. Our results showed that the interface between the tumor and the pleura is a useful MRI marker for the determination of VPSI with 91% accuracy. CT and MRI were equivalent in terms of the other parameters examined. There were no significant differences in the areas under the ROC curve between CT and MRI for the contact length, angle of mass margin, or arch distance-to-maximum tumor diameter ratio.

Elastic fiber staining is an important and widely accepted pathological technique for the detection and assessment of pleural invasion by lung cancer (31). However, a previous study has highlighted the difficulties and even the impracticality of clearly

classifying the depth of tumor invasion on histological slices when relying on identification of small and sometimes barely visible structures, such as the lamina elastica interna (35). Elastic stains may be helpful for identifying the visceral pleural surface in cases of adhered visceral and parietal pleurae (16). Although the application of elastic stains is simple and inexpensive, interpretation of the histologic results can be challenging (36). This study showed MRI to be a potential non-invasive, non-radiative adjunct for this assessment.

In this study, the free-breathing radial VIBE sequence depicted a high-signal-intensity band at the interface between the tumor and the pleura. The smoothness or irregularity of this interface distinguished tumors without and with VPSI with substantial accuracy (Figures 3, 5, and 6). This high-signal-intensity band has been shown to correspond pathologically to edematous, thickened, adhered pleura, with no parietal pleural involvement of the tumor (37). Difficulties in distinguishing tumor invasion from non-malignant, inflammatory adhesions to the pleura and chest wall have been encountered with other diagnostic approaches also, including expiratory dynamic CT (29, 38), ultrasound (39), pneumothorax CT (40), and dynamic cine MRI (33, 41). Therefore, this limitation is considered a common problem. This type of inflammatory adhesion was found on pathological examination in the two patients

with false-positive MRI findings. MRI with non-contrast T1- and T2-weighted and post-contrast pulse sequences utilized to evaluate these two patients showed an indistinct margin between the tumor and the pleura, leading to the false-positive VPSI classification (Figure 7).

A. B.

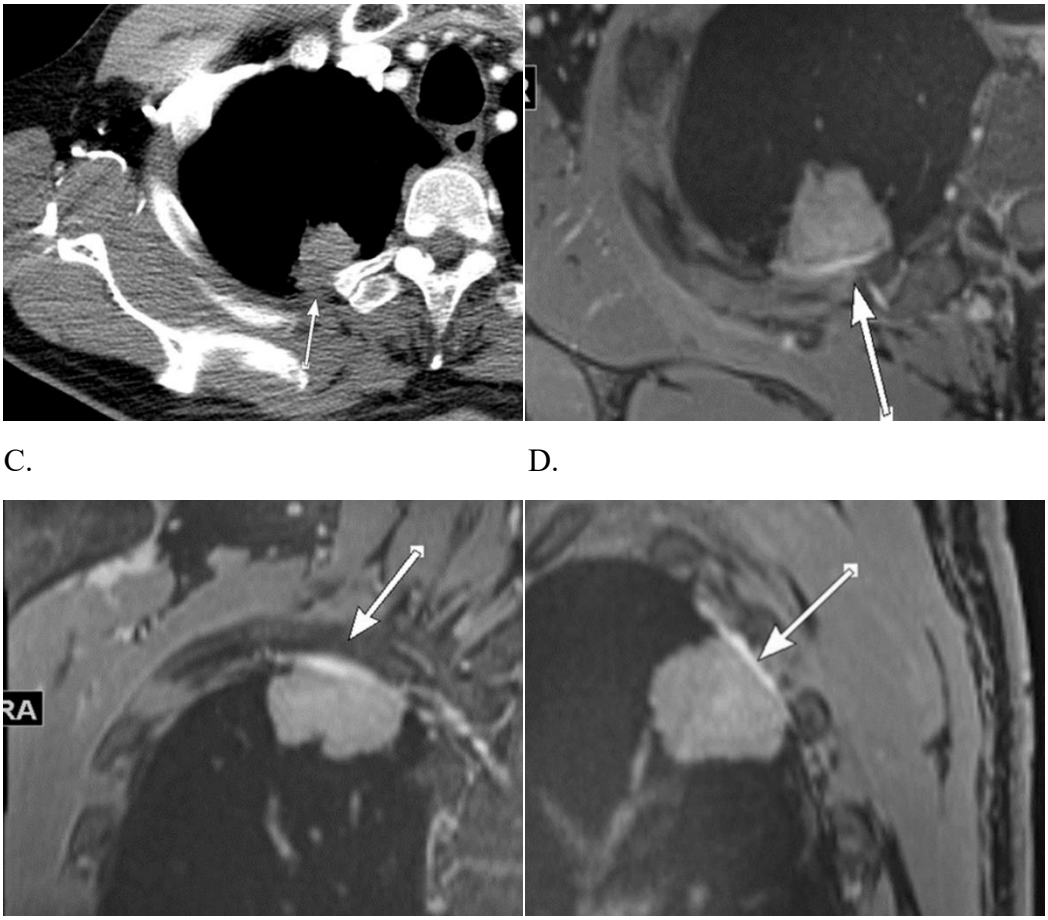

C. D.

Fig. 5. A 61-year-old man with right lower lobe lung adenocarcinoma and no visceral pleural surface invasion (PL0, as determined pathologically).

(A) Contrast-enhanced axial computed tomography (CT) shows an ambiguous, blurred interface between the tumor and the pleura (arrow) highlighting the difficulty

of evaluation of pleural invasion by CT. (B) Post-contrast free-breathing radial volumetric interpolated fat-saturated image shows a smooth and clear margin, with well-defined curvilinear pleural enhancement (arrow), and absence of protrusion at the interface between the tumor and the pleura in the axial, (C) coronal, and (D) sagittal planes. CT = computed tomography

A. B.

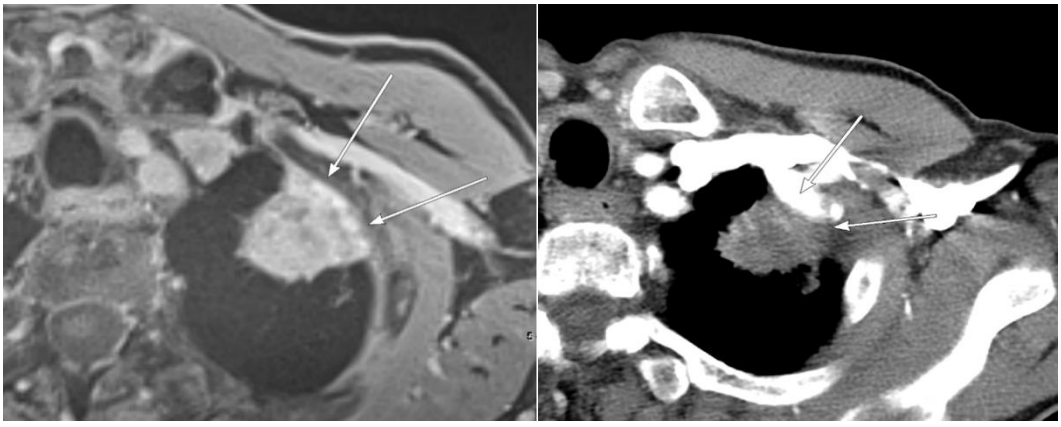

Fig. 6. A 75-year-old man with left upper lobe lung adenocarcinoma and pathologically determined visceral pleural surface invasion (PL2, as determined pathologically).

(A) Axial contrast-enhanced computed tomography (CT) does not clearly show the interface between tumor and pleura (arrow), highlighting the difficulty in evaluation of pleural invasion by CT. (B) Post-contrast radial VIBE fat-saturated image shows an irregular undulating margin (arrow) of the tumor interface with the pleura, closely abutting the intercostal muscle, and irregular thickening of the enhanced pleura adjacent to the tumor. CT = computed tomography

A.

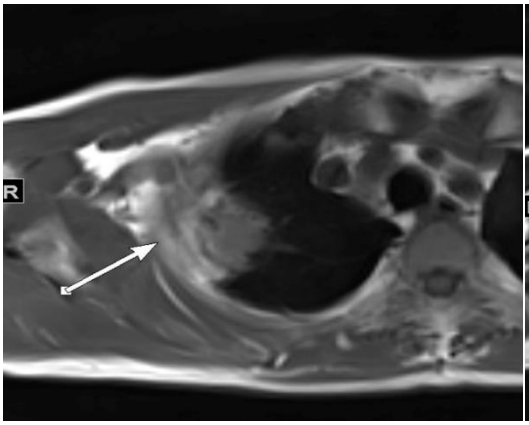

B.

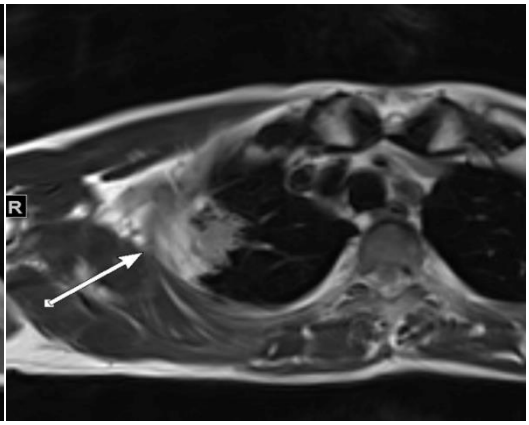

C.

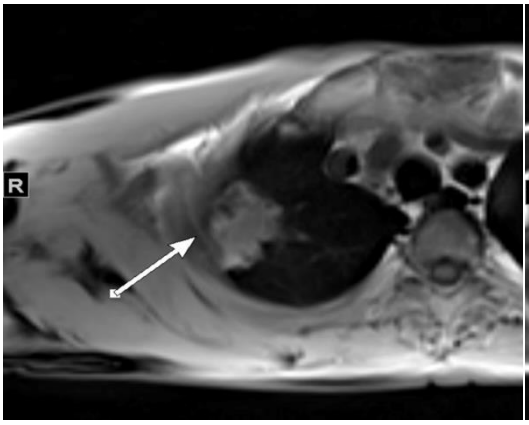

D.

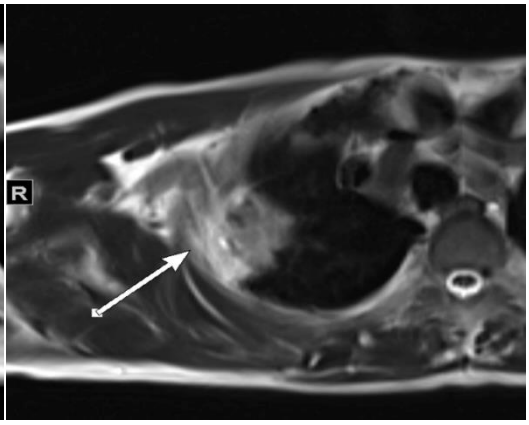

E. F.

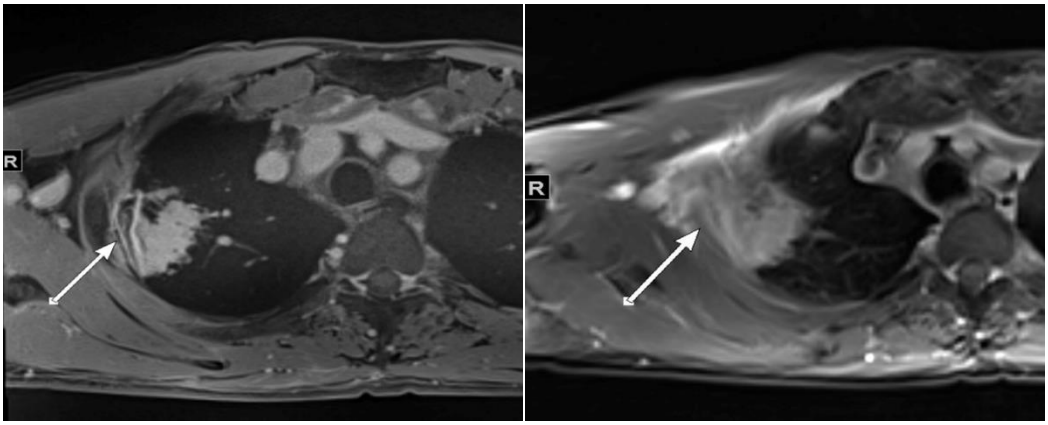

Fig. 7. A 64-year-old male with right upper lobe adenocarcinoma and no visceral pleural surface invasion (PL1, as determined pathologically).

A-C. In the non-contrast breath-hold T1-weighted (A), breath-hold T2-weighted (B), and axial fat-saturated T1-weighted breath-hold (C) images, the tumor exhibits a broad interface with the pleura (arrow) but no specific features for pleural invasion. (D) In axial T2-weighted half-Fourier acquisition single-shot turbo spin-echo and (E) axial contrast-enhanced T1-weighted fat-suppressed images, the interface between the tumor and the pleura is blurred (arrow); however, there is no obvious morphologic sign enabling distinction between visceral pleural surface invasion and the lack thereof. (F) On contrast-enhanced free-breathing radial VIBE imaging, there is a

smooth interface of the tumor with the pleura and well-defined, smooth, curvilinear pleural enhancement along the tumor (arrow).

Several other limitations should be mentioned. First, our study was retrospective in design. The diagnostic performances of other MRI pulse sequences could not be evaluated because only two pulse sequences were commonly shared among all MRI examinations. The assessment of the ability of other MRI pulse sequences to identify VPSI would be of value. Second, despite the enrollment of patients from two medical institutions, the number of patients was small, with three patients having PL2 and nine patients having PL3. This was probably because pathological proof was available only for patients who underwent an operation for a potentially resectable lung cancer. Therefore, patient selection bias was inevitable in this study. Further prospective multi-institutional studies with a larger sample size are required.

In conclusion, the diagnostic performance of contrast-enhanced radial T1-weighted gradient-echo 3T MRI and CT was equal in terms of the contact length, angle of mass

margin, and arch distance-to-maximum tumor diameter ratio. The advantage of MRI is that it can clearly show the tumor-pleura interface margin, facilitating VPSI detection. Further studies with larger sample sizes are required to verify the clinical utility of MRI for prognostic use in NSCLC patients.

List of abbreviations used

computed tomography: CT

left lower lobe：LLL

left upper lobe: LUL

magnetic resonance imaging: MRI

negative predictive value: NPV

non-small-cell lung cancer: NSCLC

Picture archiving and communication system: PACS

positive predictive value: PPV

right lower lobe: RLL

right middle lobe: RML

right upper lobe: RUL

receiver operating characteristic: ROC

3-dimensional: 3D

3-tesla:3T

volumetric interpolated breath-hold examination: VIBE

visceral pleural surface invasion: VPSI

visceral pleural invasion: VPI

REFERENCES

1. Chang YL, Lin MW, Shih JY, Wu CT, Lee YC. The Significance of Visceral Pleural Surface Invasion in 321 Cases of Non-Small Cell Lung Cancers with Pleural Retraction. Annals of surgical oncology 2012;19:3057-3064
2. Wang T, Zhou C, Zhou Q. Extent of Visceral Pleural Invasion Affects Prognosis of Resected Non-Small Cell Lung Cancer: A Meta-Analysis. Scientific Reports 2017;7:1527
3. Kawase A, Yoshida J, Miyaoka E et al. Visceral Pleural Invasion Classification in Non–Small-Cell Lung Cancer in the 7th Edition of the Tumor, Node, Metastasis Classification for Lung Cancer: Validation Analysis Based on a Large-Scale Nationwide Database. Journal of Thoracic Oncology 2013;8:606-611
4. Feng SH, Yang ST. The New 8th Tnm Staging System of Lung Cancer and Its Potential Imaging Interpretation Pitfalls and Limitations with CT Image Demonstrations. Diagnostic and interventional radiology (Ankara, Turkey) 2019;25:270-279
5. Goldstraw P, Chansky K, Crowley J et al. The Iaslc Lung Cancer Staging

Project: Proposals for Revision of the Tnm Stage Groupings in the Forthcoming (Eighth) Edition of the Tnm Classification for Lung Cancer. Journal of thoracic oncology 2016;11:39-51

6. Sakakura N, Mori S, Okuda K et al. Subcategorization of Lung Cancer Based on Tumor Size and Degree of Visceral Pleural Invasion. The Annals of thoracic surgery 2008;86:1084-1090
7. Kudo Y, Saji H, Shimada Y et al. Impact of Visceral Pleural Invasion on the Survival of Patients with Non-Small Cell Lung Cancer. Lung cancer (Amsterdam, Netherlands) 2012;78:153-160
8. Yilmaz A, Duyar SS, Cakir E et al. Clinical Impact of Visceral Pleural, Lymphovascular and Perineural Invasion in Completely Resected Non-Small Cell Lung Cancer. European journal of cardio-thoracic surgery 2011;40:664-670
9. Tanaka T, Shinya T, Sato S et al. Predicting Pleural Invasion Using Hrct and 18F-FDG PET/CT in Lung Adenocarcinoma with Pleural Contact. Annals of nuclear medicine 2015;29:757-765
10. Sugama Y, Tamaki S, Kitamura S, Kira S. Ultrasonographic Evaluation of Pleural and Chest Wall Invasion of Lung Cancer. Chest 1988;93:275-279

11. Bandi V, Lunn W, Ernst A et al. Ultrasound Vs. Ct in Detecting Chest Wall Invasion by Tumor: A Prospective Study. Chest 2008;133:881-886

12. Glazer HS, Duncan-Meyer J, Aronberg DJ et al. Pleural and Chest Wall Invasion in Bronchogenic Carcinoma: CT Evaluation. Radiology 1985;157:191-194

13. Verschakelen JA, Bogaert J, De Wever W. Computed Tomography in Staging for Lung Cancer. European Respiratory Journal 2002;19:40S-48s

14. Kawaguchi K, Mori S, Usami N et al. Preoperative Evaluation of the Depth of Chest Wall Invasion and the Extent of Combined Resections in Lung Cancer Patients. Lung cancer (Amsterdam, Netherlands) 2009;64:41-44

15. Bai JH, Hsieh MS, Liao HC, Lin MW, Chen JS. Prediction of Pleural Invasion Using Different Imaging Tools in Non-Small Cell Lung Cancer. Annals of translational medicine 2019;7:33

16. Shimada Y, Yoshida J, Hishida T et al. Predictive Factors of Pathologically Proven Noninvasive Tumor Characteristics in T1an0m0 Peripheral Non-Small Cell Lung Cancer. Chest 2012;141:1003-1009

17. Suzuki K, Koike T, Asakawa T et al. A Prospective Radiological Study of Thin-Section Computed Tomography to Predict Pathological Noninvasiveness in

Peripheral Clinical Ia Lung Cancer (Japan Clinical Oncology Group 0201). Journal of thoracic oncology 2011;6:751-756

18. Ebara K, Takashima S, Jiang B et al. Pleural Invasion by Peripheral Lung Cancer: Prediction with Three-Dimensional CT. Academic radiology 2015;22:310-319

19. Hsu JS, Han IT, Tsai TH et al. Pleural Tags on CT Scans to Predict Visceral Pleural Invasion of Non-Small Cell Lung Cancer That Does Not Abut the Pleura. Radiology 2016;279:590-596

20. Hsu JS, Jaw TS, Yang CJ et al. Convex Border of Peripheral Non-Small Cell Lung Cancer on CT Images as a Potential Indicator of Pleural Invasion. Medicine 2017;96:e7323

21. Cho HH, Choi YH, Cheon JE et al. Free-Breathing Radial 3d Fat-Suppressed T1-Weighted Gradient-Echo Sequence for Contrast-Enhanced Pediatric Spinal Imaging: Comparison with T1-Weighted Turbo Spin-Echo Sequence. AJR. American journal of roentgenology 2016;207:177-182

22. Zhang F, Qu J, Zhang H et al. Preoperative T Staging of Potentially Resectable Esophageal Cancer: A Comparison between Free-Breathing Radial Vibe and Breath-Hold Cartesian Vibe, with Histopathological Correlation. Translational

oncology 2017;10:324-331

23. Chandarana H, Block TK, Rosenkrantz AB et al. Free-Breathing Radial 3d Fat-Suppressed T1-Weighted Gradient Echo Sequence: A Viable Alternative for Contrast-Enhanced Liver Imaging in Patients Unable to Suspend Respiration. Investigative radiology 2011;46:648-653

24. Bamrungchart S, Tantaway EM, Midia EC et al. Free Breathing Three-Dimensional Gradient Echo-Sequence with Radial Data Sampling (Radial 3d-Gre) Examination of the Pancreas: Comparison with Standard 3d-Gre Volumetric Interpolated Breathhold Examination (Vibe). Journal of magnetic resonance imaging : JMRI 2013;38:1572-1577

25. Biederer J, Graessner J, Heller M. Magnetic Resonance Imaging of the Lung with a Volumetric Interpolated 3d-Gradient Echo Sequence. RoFo : Fortschritte auf dem Gebiete der Rontgenstrahlen und der Nuklearmedizin 2001;173:883-887

26. Biederer J, Both M, Graessner J et al. Lung Morphology: Fast Mr Imaging Assessment with a Volumetric Interpolated Breath-Hold Technique: Initial Experience with Patients. Radiology 2003;226:242-249

27. Lee H, Choi E, Lee MK, Zhang Y, Kwon W. Morphologic Evaluation of

Primary Non-Small Cell Lung Cancer by 3 Tesla Mri with Free-Breathing Ultrashort Echo Time and Radial T1-Weighted Gradient Echo Sequences: A Comparison with Ct Analysis. J Korean Soc Radiol 2019;80:466-476

28. Herman SJ, Winton TL, Weisbrod GL, Towers MJ, Mentzer SJ. Mediastinal Invasion by Bronchogenic Carcinoma: CT Signs. Radiology 1994;190:841-846

29. Glazer HS, Kaiser LR, Anderson DJ et al. Indeterminate Mediastinal Invasion in Bronchogenic Carcinoma: CT Evaluation. Radiology 1989;173:37-42

30. Imai K, Minamiya Y, Ishiyama K et al. Use of CT to Evaluate Pleural Invasion in Non-Small Cell Lung Cancer: Measurement of the Ratio of the Interface between Tumor and Neighboring Structures to Maximum Tumor Diameter. Radiology 2013;267:619-626

31. Travis WD, Brambilla E, Rami-Porta R et al. Visceral Pleural Invasion: Pathologic Criteria and Use of Elastic Stains: Proposal for the 7th Edition of the Tnm Classification for Lung Cancer. Journal of thoracic oncology 2008;3:1384-1390

32. Kundel HL, Polansky M. Measurement of Observer Agreement. Radiology 2003;228:303-308

33. Akata S, Kajiwara N, Park J et al. Evaluation of Chest Wall Invasion by Lung

Cancer Using Respiratory Dynamic MRI. Journal of medical imaging and radiation oncology 2008;52:36-39

34. Tsuchiya N, Doai M, Usuda K, Uramoto H, Tonami H. Non-Small Cell Lung Cancer: Whole-Lesion Histogram Analysis of the Apparent Diffusion Coefficient for Assessment of Tumor Grade, Lymphovascular Invasion and Pleural Invasion. PloS one 2017;12:e0172433

35. Warth A, Muley T, Herpel E et al. A Histochemical Approach to the Diagnosis of Visceral Pleural Infiltration by Non-Small Cell Lung Cancer. Pathology oncology research : POR 2010;16:119-123

36. Gallagher B, Urbanski SJ. The Significance of Pleural Elastica Invasion by Lung Carcinomas. Human pathology 1990;21:512-517

37. Shiotani S, Sugimura K, Sugihara M et al. Diagnosis of Chest Wall Invasion by Lung Cancer: Useful Criteria for Exclusion of the Possibility of Chest Wall Invasion with Mr Imaging. Radiation medicine 2000;18:283-290

38. Murata K, Takahashi M, Mori M et al. Chest Wall and Mediastinal Invasion by Lung Cancer: Evaluation with Multisection Expiratory Dynamic Ct. Radiology 1994;191:251-255

39. Suzuki N, Saitoh T, Kitamura S. Tumor Invasion of the Chest Wall in Lung

Cancer: Diagnosis with Us. Radiology 1993;187:39-42

40. Yokoi K, Mori K, Miyazawa N et al. Tumor Invasion of the Chest Wall and Mediastinum in Lung Cancer: Evaluation with Pneumothorax Ct. Radiology 1991;181:147-152

41. Kajiwara N, Akata S, Uchida O et al. Cine Mri Enables Better Therapeutic Planning Than Ct in Cases of Possible Lung Cancer Chest Wall Invasion. Lung cancer (Amsterdam, Netherlands) 2010;69:203-208

ABSTRACT IN KOREAN(국문요약)

폐암의 장측 흉막 표면 침범에 대한 평가: CT 와 방사형 T1 강조영상 경사에코 3T MR 영상비교

장옥(Yu Zhang)

연세대학교 대학원 의학과

<지도교수: 고성민>

목적 : 내장 흉막 표면 침윤 (VPSI)의 검출을 위한 조영 강화 방사형 T1 가중 그라데이션 에코 3-테슬라(3T) 자기 공명 영상(MRI)와 컴퓨터 단층 촬영 (CT)의 진단 성능을 비교하고자 합니다. 비소 세포 폐암 (NSCLC)에 의한 장측 흉막 침범은 PL1 (VPSI 없음) 장측 흉막 표면에 도달하지 않는

장측 흉막의 탄성 층에 침범 및 PL2 (VPSI 있음)의 2 가지 유형으로 분류할 수 있습니다, 내장 흉막의 완전한 침범.

재료 및 방법 : NSCLC 에 의해 병리학 적으로 VPSI 이 확인 된 33 명의 환자를 후향적으로 검토했습니다. 다중 검출기 CT 와 자유 호흡의 방사형 3 차원 지방 억제 체적 보간 숨 방지 검사 (VIBE) 펄스 시퀀스를 갖춘 조영제 증강 3T MRI 를 종양와 흉막사이의 접촉길이, 종양와 흉막사이의 각도 및 접촉길이 와 최대 종양 직경 의 비율 비교 했습니다. 종양과 침범 사이의 계면의 형태를 평가 (매끄럽거나 불규칙한지 여부)은 MRI 에서만 실행할 수 있었습니다 (CT 에서 식별 할 수 없습니다).

결과 : 종양 - 흉막 침범 사이의 계면에서 방사형 VIBE MRI 는 VPSI 없는 21 명의 환자 중 20 명에서 매끄러운 형태를 보이고 VPSI 있는 12 명의

환자 중 10 명에서 불규칙한 형태를 보입니다. 정확도, 민감도, 특이도, 양성 예측치, 음성 예측치 및 F 점수는 각각 91 %, 83 %, 95 %, 91 %, 91 % 및 87 %입니다. McNemar 검정 및 수신자 동작 특성 곡선 분석에서는 VPSI 의 예측 인자로서 종양와 흉막사이의 접촉길이, 종양와 흉막사이의 각도 및 접촉길이 와 최대 종양 직경 의 비율에서 CT 와 MRI 의 진단 정확도는 큰 차이가 없습니다.

결론 : 조영 강화 방사형 T1 가중 그라데이션 에코 3T MRI 및 CT 의 진단 성능은 종양와 흉막사이의 접촉길이, 종양와 흉막사이의 각도 및 접촉길이 와 최대 종양 직경 의 비율에서 비슷합니다. MRI 의 장점은 종양과 흉막의 경계면이 명확하게 묘사되어 VPSI 의 검출이 용이하게 될 것입니다.